Key Features of Bolaamphiphile Structures for the Synthesis, Stabilization, and Catalytic Properties of Gold Nanoparticles

Stéphanie Sistach, Elodie Marinoni, Christophe Mingotaud, Nancy Lauth-de Viguerie, Jean-Daniel Marty

THE JOURNAL OF PHYSICAL CHEMISTRY C
A JOURNAL OF THE AMERICAN CHEMICAL SOCIETY

pubs.acs.org/JPCC

Article

Key Features of Bolaamphiphile Structures for the Synthesis, Stabilization, and Catalytic Properties of Gold Nanoparticles

Stéphanie Sistach, Elodie Marinoni, Christophe Mingotaud, Nancy Lauth-de Viguerie,* and Jean-Daniel Marty*

Cite This: *J. Phys. Chem. C* 2022, 126, 11051−11057

Read Online

ACCESS | Metrics & More | Article Recommendations | Supporting Information

ABSTRACT: Bolaamphiphilic-type structures can be effective substitutes to conventional surfactants for the interaction and stabilization of colloidal interfaces in water. Different families of bolaamphiphiles were used as a growth control and stabilizing agent for the formation of gold nanoparticles (AuNPs). The nature of polar heads and the length of hydrophobic chain are key parameters for modulating the interaction with gold surfaces. In particular, interactions between hydrophobic chains dramatically strengthen the interactions with NP surfaces leading to a reversible aggregation process. This affects not only the gold nanoparticle growth mechanism and stabilization properties but also the catalytic properties of the modified gold nanoparticles.

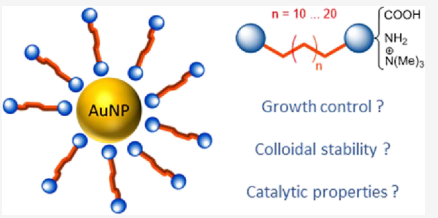

1. INTRODUCTION

The synthesis and stabilization of nanoparticles (NPs) require the use of organic compounds, some of which act as structuring agents to control the NP synthesis and others as agents to ensure colloidal stability in a chosen solvent. In this context, surfactant molecules have been widely used. For example, the synthesis of gold NPs of controlled size and morphology has greatly benefited from the use of cetyltrimethylammonium bromide. The latter forms an interdigitated layer on the surface of the NPs that controls the growth of gold nanorods and ensures colloidal stability in aqueous solution.[1,2] By analogy, the use of surfactants bearing two polar heads connected by a hydrophobic chain, known as bolaamphiphiles or bolaform surfactants, should be molecules of choice. Thus, some studies have shown in the past the potential of these structures to act as a template for the synthesis of NPs[3,4] and to direct the self-assemblies of NPs[5] or for the modification of interfaces and the stabilization of AuNPs[6−10] or nanostructures.[11] The important role of the hydrophobic chain length in the stabilization of preformed NPs has been highlighted: a long chain length favors the stabilization of NPs.[6] However, these studies remain limited, and many questions remain regarding the role of heads and chain lengths and the possibility of tuning the properties of stabilized NPs.

The objective of this article is to rationalize the effect of the structure of the bolaamphiphile (nature of the head and role of the hydrophobic part) not only on the possibility of stabilizing preformed NPs but also on its ability to act as a control agent for the in situ synthesis of NPs and to link this effect to the catalytic properties of the formed NPs.

2. EXPERIMENTAL SECTION

2.1. Materials. Solvents (Prolabo or Carlo Erba) were dried prior to use according to standard methods.[12,18] All aqueous solutions were prepared with ultrapure water (Purite device, resistivity ≈ 18 MΩ cm). The reagents were purchased from Aldrich or Acros or Fluka or TCI (>98% purity) and were used as received. 1,12-Dodecanedioic acid (BolaCOOH-C_{12}) and 1,12-dodecanediamine (BolaNH_2-C_{12}) were purchased from Aldrich. Sodium borohydride ($NaBH_4$) and hydrogen tetrachloroaurate(III) trihydrate (99% purity) were purchased from Acros.

2.2. General Procedure. FTIR spectra were recorded in the ATR mode using a Nexus Thermo Nicolet spectrophotometer equipped with an ATR diamond crystal and on a PerkinElmer IRFT 1760-X spectrophotometer. Mass spectra were recorded on a Waters Qtof Ultima API apparatus. ^1H and ^{13}C NMR spectra were recorded on a Bruker ARX 300 spectrometer at 300.13 MHz and at 75.47 MHz, respectively. Nuclear overhauser effect (NOE) experiments were recorded on a Bruker ARX 500 spectrometer equipped with a cryoprobe. UV−visible spectra were measured on a diode array (Hewlett Packard 8452) or a double beam (Varian Cary 100 bio), equipped with a temperature control system and magnetic stirring. For transmission electron microscopy (TEM), a drop of solution was placed on a formvar carbon-coated copper TEM grid (200 mesh, Ted Pella, Inc.) and left to dry at room

Received: March 4, 2022
Revised: June 15, 2022
Published: June 29, 2022

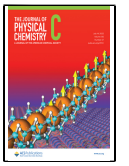

https://doi.org/10.1021/acs.jpcc.2c01545
J. Phys. Chem. C 2022, 126, 11051−11057

temperature. The samples were viewed with a Hitachi HU12 microscope operating at a 70 keV accelerating voltage. The size distribution of the particles was determined using WCIF ImageJ software, and confidence intervals were given as the average diameter ± standard deviation. An aqueous solution of uranyl acetate (2 wt %, 2 min) was used for negative staining.

2.3. Bolaamphiphile Synthesis. *2.3.1. Synthesis of BolaAla-C_n.* The synthesis of BolaAla-C_n with n = 10, 12, 14, 16, 18, and 20 was performed as previously described (Scheme S1 in the SI).[6,13]

2.3.2. Synthesis of BolaNMe$_3^+$-C_{12}. *N,N,N,N′,N′,N′*-Hexamethyl 1,20-dodecanediammonium dibromide was synthesized from 1,12-dibromooctane and anhydrous trimethylamine according to the Menger protocol (Scheme S2 in the SI).[14]

2.3.3. Synthesis of BolaNMe$_3^+$-C_{20}. *N,N,N,N′,N′,N′*-Hexamethyl 1,20-eicosanediammonium dibromide was synthesized from 1,20-dibromoeicosane and anhydrous trimethylamine (Scheme S3 in the SI).[14] 1,20-Dibromoeicosane was formed by assembling C6 and C8 units as described by Jablonkai and Oroszlan[15] in which 1,8-octanedimagnesium chloride (Grignard reagent) reacts with 1,6-dibromohexane in the presence of lithium tetrachlorocuprate(II).

2.3.4. Synthesis Route of BolaAlaR-C_{12}. Its synthesis was obtained in a two-step synthetic pathway from the addition of Boc-L-alanine to 1,12-diaminododecane followed by a deprotection step of the Boc group by addition of gaseous HCl (Scheme S4 in the SI).

2.4. CAC Determination by Surface Tension. Surface tension measurements for BolaAla-C_{10}, BolaAla-C_{12}, and BolaAlaR-C_{12} were performed using a Krüss EasyDyne tensiometer using the Wilhelmy plate method. Temperatures were maintained at 20 or 30 °C (±0.1 °C) by circulating thermostated water through a jacketed vessel containing the solution. For each experiment, surface tension was measured three times (each time, 10 readings were performed and averaged). Surface tension measurements for BolaAla-C_{14}, BolaAla-C_{16}, BolaAla-C_{18}, BolaAla-C_{20}, and BolaNMe$_3^+$ were performed with a pendent drop tensiometer (Krüss GmbH, model DSA 10-MK2, Germany). Temperatures were maintained at 20 or 30 °C (±0.1 °C) by circulating thermostated water. The diameter of the needle was 1.463 mm. All measurements were made until three concordant values were obtained (difference of less than 0.2 mN m^{-1}). Standard deviation was calculated on the basis of these three measurements. Fitting was obtained by using the Szyszkowski−Langmuir adsorption model (Figures S1−S3 in the SI).

2.5. Stabilization of Preformed AuNPs. *2.5.1. Synthesis of Preformed AuNPs.* The synthesis of the gold NPs was performed as previously described.[6] The UV−visible absorption spectrum and the TEM image with corresponding diameter distribution are given in Figure S5 in the SI. In the following, the given gold concentrations correspond to the atomic concentration of gold.

2.5.2. Influence of Head Groups. Stock aqueous solutions of BolaAla-C_{12}, BolaAlaR-C_{12}, BolaNH$_2$-C_{12}, BolaCOOH-C_{12}, and BolaNMe$_3^+$-C_{12} at 10^{-3} mol·L^{-1} and a stock solution of preformed AuNPs at 5×10^{-4} mol·L^{-1} were prepared separately. For each bolaamphiphile, 12 aliquots were prepared containing 1 mL of aqueous gold NP solution and 500 μL of bolaamphiphile solution. The pH was then changed by adding variable volumes of 0.1 mol·L^{-1} HCl or mol·L^{-1} NaOH solution to obtain pH ranges from about 2 to 11. Then, the total volume was adjusted to 2 mL with a NaCl solution (0.1 mol·L^{-1}) to achieve a constant ionic strength in all samples. It was observed that some samples changed in color from red to violet or blue or precipitated. Evolution of the absorbance spectra with time of each solution was studied as described in SI Section III.2 (Figure S6) to extract the maximum flocculation parameters (FP$_{max}$). For each family, FP$_{max}$ values were then plotted as a function of pH.

2.5.3. Influence of the Hydrophobic Chain Length. To aliquots containing 200 μL of aqueous solutions of BolaAla-C_n at 10^{-3} mol·L^{-1}, 800 μL of solution of preformed AuNPs at 5×10^{-4} mol·L^{-1} and 1.5 mL of water were added along with 20 μL of HCl at 1 mol·L^{-1}. Photographs were taken after 5 min and 2 h. After 24 h, 20 μL of NaOH at 1 mol·L^{-1} was added. The sample was sonicated for 30 s, and photographs were taken after 5 min (Figure S7 in the SI). Additionally, stock aqueous solutions of BolaAla-C_n at 2×10^{-3} mol·L^{-1} and a stock solution of preformed AuNPs at 5×10^{-4} mol·L^{-1} were prepared. Aliquots containing 50 μL of aqueous solutions of BolaAla-C_n (final concentration from 4×10^{-5} mol·L^{-1}), 1000 μL of preformed AuNPs, and water to have a final volume of 2500 μL were prepared. The pH was then changed to 2 by adding 0.1 mol·L^{-1} HCl aqueous solution. The evolution of the absorbance spectra of each solution was recorded between 400 and 800 nm at timed intervals (for example, see Figure S8 for pristine AuNPs (A), AuNPs@BolaAla-C_{10}, AuNPs@BolaAla-C_{14}, and AuNPs@BolaAla-C_{20}). The spectra obtained at each time were treated as described in Section 2.5.2 (normalization and integration) to obtain the values of the flocculation parameter (FP).

2.5.4. Influence of the Concentration of BolaAla-C_n on Redispersibility of the System. Stock aqueous solutions of BolaAla-C_n at 2×10^{-3} mol·L^{-1} and a stock solution of preformed AuNPs at 5×10^{-4} mol·L^{-1} were prepared separately. Aliquots containing variable volumes of aqueous solutions of BolaAla-C_n from 2 to 400 μL (final concentration from 0.16 to 32×10^{-5} mol·L^{-1}), 1000 μL of preformed AuNPs, and water to have a final volume of 2500 μL were prepared (A). Then, NPs were destabilized by adding 20 μL of HCl at 1 mol·L^{-1}. The photographs were taken 24 h after the addition of acid solution (B). Then, an aqueous solution of NaOH at 1 mol·L^{-1} was added until the pH was 7. The sample was sonicated for 30 s, and photographs were taken after 5 min (C) (Figure S9 in the SI). The evolution of the flocculation parameter for the previous colloidal solutions (at different concentrations in BolaAla-C_n) after destabilization by adding hydrochloride solution was followed as a function of time. The plots obtained for NPs@BolaAla-C_{10} and NPs@BolaAla-C_{20} are given in Figure S10 in the SI.

2.5.5. Salt Effect. Stock aqueous solutions of BolaAla-C_n, preformed AuNPs at 5×10^{-4} mol·L^{-1}, and NaCl were prepared separately. These solutions were mixed together so that the final concentrations of the different components are as follows: [Au] = 2×10^{-4} mol·L^{-1}, [NaCl] = 0.06 mol·L^{-1}, and BolaAla-C_n varied from 0.4 to 4.8×10^{-5} mol·L^{-1}. The evolution of spectra was followed through time (Figure S11 in the SI).

3. RESULTS AND DISCUSSION

Symmetrical bolaamphiphiles bearing different head groups were used and are depicted in Figure 1: three with amine or ammonium functions (BolaNH$_2$, BolaNMe$_3^+$, and BolaAlaR) and two with acidic functions (BolaCOOH and BolaAla).[13]

https://doi.org/10.1021/acs.jpcc.2c01545
J. Phys. Chem. C 2022, 126, 11051−11057

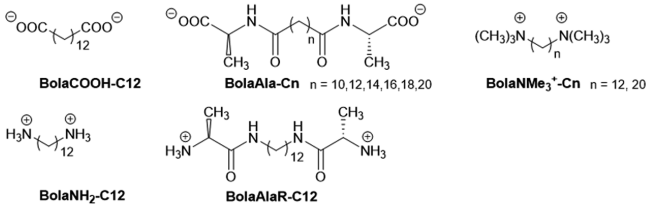

Figure 1. Structures of bolaamphiphiles used in this study to stabilize AuNPs (chloride and sodium counterions have not been represented).

The number of carbon atoms, *n*, in the hydrophobic spacers was also changed for some of these families (*n* = 10, 12, 14, 16, 18, and 20 carbon atoms). Like usual surfactants, bolaamphiphiles have the ability to self-organize in aqueous solution. Their behaviors in water solution were studied by tensiometry and transmission electron microscopy (TEM). Surface tension measurements (Figures S1−S3 in the SI) were performed to determine the critical aggregation concentration (CAC). The area per molecule at the air/water interface was estimated by fitting the tensiometry curve by using the Szyszkowski−Langmuir adsorption equation,[16] and the results are summarized in Table 1. Above the CAC, the formation of highly ordered structures promoted by amide functions such as fibers or vesicles can be evidenced by TEM (see Table 1 and examples in Figure S4).

Table 1. Characteristics of Studied Bolaamphiphiles[d]

bolaamphiphile	CAC (mol·L^{-1})	molecular area (Å^2)	ΔG** (kcal/mol)	nature of aggregate
BolaAla-C_{10}	>0.1[a]*	55	−4.5	vesicles (50 nm)
BolaAla-C_{12}	0.005[a]*	41	−4.6	vesicles (60 nm)
				twisted fibers
BolaAla-C_{14}	>0.2[b]	116	−4.9	n.d.
BolaAla-C_{16}	>0.2[b]	81	−4.7	n.d.
BolaAla-C_{18}	0.0025[b]	28	−5.6	n.d.
BolaAla-C_{20}	0.0018[b]	106	−5.0	micelles
	0.002[a]*			
BolaNMe$_3^+$-C_{12}	1.64[c]*	61	−4.4	aggregates
BolaNMe$_3^+$-C_{20}	0.01[b]	76	−5.1	micelles
	0.0085[c]			
BolaAlaR-C_{12}	>0.01[a]	n.d.	n.d.	n.d.

[a]30 °C. [b]20 °C. [c]25 °C. [d]*: From the literature; n.d.: not determined. **: The values of Gibbs energy adsorption at the air−water interface were calculated using $\Delta G = -RT \times \ln(d\pi/dC)$ as $C \rightarrow 0$ where π is the difference of surface tension at the air−water interface between water and a solution of surfactant at a given concentration. Estimated standard deviation for CAC = $\pm 10^{-3}$ mol·L^{-1}, area = ±5 Å^2, and ΔG = ±0.5 kcal·mol^{-1}.

These families of bolaamphiphiles are then studied for their ability to stabilize preformed AuNPs synthesized by reduction of $HAuCl_4$ by $NaBH_4$ (Figure S5 in the SI). These preformed AuNPs have an average diameter of 7.9 ± 2.3 nm with a negative zeta potential and are sensitive to any external stimulus (change in pH and addition of salt), which induces charge neutralization/screening and flocculation/aggregation phenomena.

When a solution of bolaamphiphiles was added to preformed AuNPs at a chosen concentration, the maximum of the surface plasmon band of the pristine NPs at 520 nm was slightly shifted to a higher wavelength suggesting interactions between the bolaamphiphiles and the NP surface. In addition, the absorbance spectra of these solutions were recorded versus time to get information on their colloidal stability. Indeed, when a flocculation or an aggregation phenomenon occurred, the global aspect of the spectra progressively changed through time and a second band related to particle aggregation appeared at higher wavelengths. This is illustrated in Figure 2A in the case of BolaAla-C_{12} when the pH of the solution

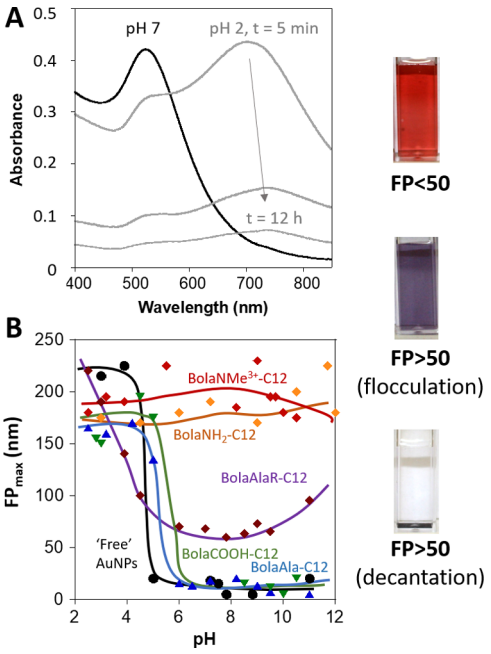

Figure 2. (A) Evolution of the absorbance as a function of time after pH adjustment to 2 (BolaAla-C_{12}). (B) Flocculation parameter FP_{max} as a function of pH for bolaamphiphiles bearing different polar heads with a C_{12} hydrophobic part ([Au] = 2.5 × 10^{-4} mol·L^{-1} and [bolaamphiphiles] = 2.5 × 10^{-4} mol·L^{-1}). The photographs on the right illustrate how the value of the flocculation parameter affects the state of the AuNPs solutions.

initially equal to 7 was adjusted to 2. In this example, a decantation phenomenon also occurred that led progressively to a decrease in intensity of the overall spectra.

In order to analyze quantitatively these results, a semi-empirical flocculation parameter (FP) was calculated.[17] The latter was measured from normalized spectra by calculating the integration between 600 and 800 nm from which the integrated absorption for pristine AuNPs was subtracted (see Section IV.2 and Figure S6 in the SI).[18−20] The normalization step enables us to get rid of the decantation phenomenon. For a given solution, the FP increases through time to reach a plateau. The experimental kinetic data were analyzed by fitting the flocculation parameter to a monoexponential equation (eq 1):

$$FP = FP_{max}(1 - \exp(-t/\tau_F)) \quad (1)$$

where FP_{max} represents the plateau value and τ_F is a characteristic time describing the kinetics of the absorption changes.[20]

For each family of bolaamphiphiles comprising a C_{12} alkyl chain, different solutions were prepared for the range of pH from 2 to 12 while keeping the concentration of gold and

https://doi.org/10.1021/acs.jpcc.2c01545
J. Phys. Chem. C 2022, 126, 11051−11057

bolaamphiphiles constant at 2.5 × 10^{-4} mol·L^{-1}. For each solution, the FP_{max} was determined as previously described. Figure 2B depicts the evolution of the FP_{max} as a function of pH for bolaamphiphiles used as a coating agent comprising 12 atoms of carbon (C_{12}) with different polar heads but a constant bolaamphiphile concentration.

Whatever the pH may be, for amine- or ammonium-based bolaamphiphiles (BolaNH$_2$, BolaNMe$_3^+$, and BolaAlaR), FP values remain higher than 50. As illustrated in Figure 2 (right), such values correspond to a flocculation or aggregation phenomenon. These families are thus not suitable for the stabilization of AuNPs. For naked particles and structures with acid functions (BolaAla and BolaCOOH), high values of the flocculation parameter were only measured for low pH values, i.e., below the pK_a value of the carboxylic functions: polar heads are present in their acidic form, thus promoting the formation of hydrogen bonds between nanohybrids and inducing progressively their aggregation. This range of pH is therefore not suitable to obtain good colloidal stability. Above pH 5 (i.e. above pK_a), low flocculation parameters and a zeta potential value of around −40 ± 5 mV were measured: carboxylate functions promoted the interactions with the surface of pristine AuNPs and prevented the aggregation of obtained hybrid nanoparticles.

To further assess the effect of the hydrophobic chain length, a second set of experiments was conducted with L-alanine-based bolaamphiphiles comprising different lengths of the alkyl chain BolaAla-C_n. First, to assess the effect of concentration on the colloidal stability of the AuNPs, bolaamphiphiles were added at different concentrations upon preformed AuNPs at pH 7. Then, the pH of the solution was adjusted upon these solutions by addition of HCl or NaOH (Figure 3 and Figures S7−S10 in the SI), and the evolution of absorption spectra was recorded through time. The effect of the hydrophobic chain length at a concentration of 8 × 10^{-5} mol·L^{-1} is first considered (Figures S7 and S8 in the SI). In the case of BolaAla-C_{10} and C_{12}, the absorbance spectra of the solutions present a supplementary band as illustrated in Figures 2A and 3A resulting in a change of color of the solution. Lowering the pH to acidic conditions (around 2) induced an irreversible aggregation of NPs. For longer chains (C_{16}, C_{18}, and C_{20}), a good redispersibility is observed when after acidification, the pH is returned to 7 with no modification of measured absorbance and no change of the observed color (Figure 3A). Interestingly, at the same time, the decantation induced by the lowering of pH does not lead to the appearance of a second plasmon band (Figure S8 in the SI).

Figure 3B further illustrates the effect of concentration on the stabilization capacity of preformed NPs. In the case of BolaAla-C_{10} and C_{12}, whatever the concentration may be, lowering the pH to acidic conditions induced an irreversible aggregation of NPs with high FP_{max} values. For longer chains (C_{16}, C_{18}, and C_{20}), a good redispersibility is observed for concentrations higher than 10^{-4} mol·L^{-1} when after acidification, the pH is returned to 7 (Figure 3A,B and Figures S9 and S10 in the SI). This minimum concentration is well below the respective CAC of the different bolaamphiphiles (Table 1) and leads to a sufficient coverage of AuNPs. In addition, a good colloidal stability is also observed upon addition of NaCl in that case (Figure S11 in the SI). Moreover, the effect observed on bolaamphiphiles with L-alanine heads is also observed on structures with ammonium heads. Hence, in the case of BolaNMe$_3^+$, whereas BolaNMe$_3^+$-C_{12} does not lead to

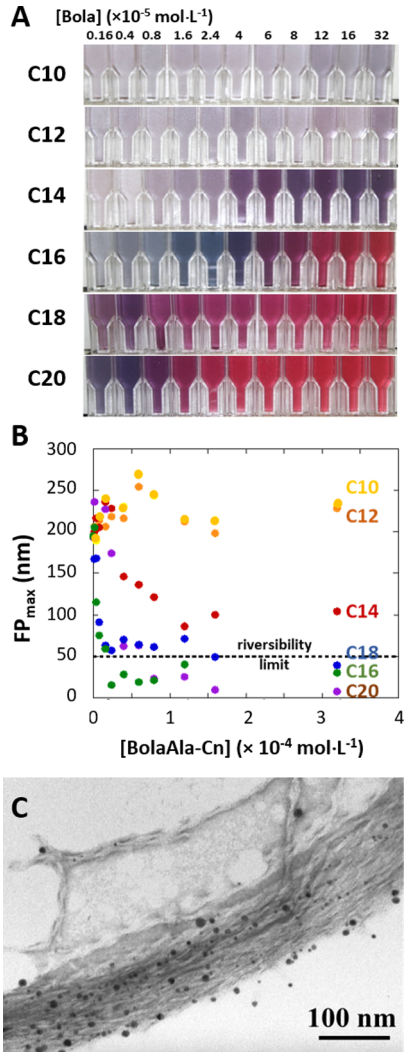

Figure 3. (A) Redispersion of solution of AuNPs@BolaAla-C_n first precipitated at pH 2 and then redispersed at pH 7 by addition of NaOH (photos taken after addition of NaOH and 5 min of sonication). The numbers shown at the top of the figure correspond to the concentrations of BolaAla-C_n ([Au] =2.5 × 10^{-4} mol·L^{-1}). (B) Flocculation parameter FP_{max} as a function of [BolaAla-C_n] for n = 10−20. (C) TEM image of precipitates obtained after decreasing the pH down to 2 for AuNPs@BolaAla-C_{20}.

stable colloidal solutions, BolaNMe$_3^+$-C_{20} improves significantly the colloidal stability of corresponding nanohybrids at pH 7 (Figure S12 in the SI). Thus, this set of experiments illustrates also the striking effect of the hydrophobic chain length upon colloidal stabilization properties, which has been previously described to play a critical role in the level of interactions with NPs: the longer the chain, the higher the stability of the adsorbed organic layer on the NP surface.[6]

To get further insights into the mechanism behind these observations, NMR and electron microscopy experiments were then performed on BolaAla-C_n. By NMR, no exchange-transferred NOE transfer was measured on the signal of bolaamphiphiles: thus, we assume that on the timescale of NMR, no exchange between the NP surface and bolaamphiphiles takes place in solution. Based on this result, the amount of free bolaamphiphiles present in solution was evaluated for different concentrations of bolaamphiphiles added on a constant concentration of AuNPs. From this, an apparent

https://doi.org/10.1021/acs.jpcc.2c01545
J. Phys. Chem. C 2022, 126, 11051−11057

equilibrium constant relative to the adsorption of bolaamphiphiles onto the surface of AuNPs is calculated (see Figures S13 and S14 in the SI). This constant is equal to zero for BolaAla-C_{10} and C_{12}. For structures comprising a longer alkyl chain, increasing values were measured at 4000 ± 2000, 9500 ± 2000, and 8300 ± 1500 for BolaAla-C_{14}, C_{16}, and C_{20}, respectively. TEM images of precipitates obtained in the case of bolaamphiphiles with the shorter chain length present only aggregated NPs (see Figure S15 in the case of BolaAla-C_{12} in the SI). On the contrary, as illustrated in Figure 3C in the case of BolaAla-C_{20}, precipitates issued for the bolaamphiphiles with longer chains present loose structures made of helicoidal structures and AuNPs trapped within. These structures, which occurred also in the absence of NPs,[13] originated from the precipitation of BolaAla-C_{20} at a low pH.

These results enable us to propose the following mechanism illustrated in Figure 4: for short hydrophobic chain lengths, the

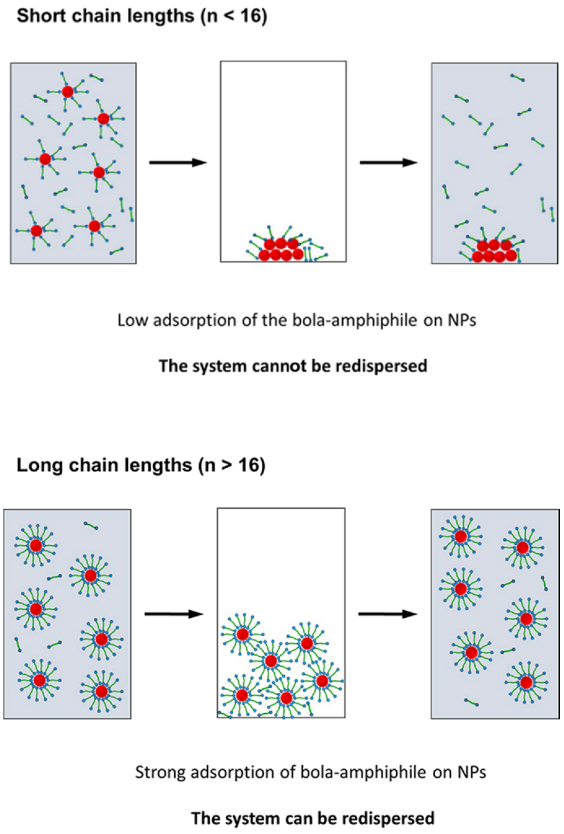

Figure 4. Proposed mechanism of redispersion depending on the alkyl chain length.

interaction of the bolaamphiphile with the surface of the nanoparticles is weak. Addition of salt or a change in pH induces desorption of the stabilizer and irreversible precipitation of AuNPs. On the contrary, for longer hydrophobic chain lengths, the interaction of the bolaamphiphile with the gold surface becomes significantly more important, and a change in pH or ionic strength is no longer sufficient to induce its desorption.

Thus, the passage below the characteristic pK_a value of the bolaamphiphile induces the cocrystallization of the bolaamphiphile and AuNPs coated with this bolaamphiphile. Since the environment of the NPs changes only slightly, no additional plasmon bands appear on the adsorption spectra. A rise in pH therefore induces the solubilization of the bolaamphiphile and the redispersion of NPs taken up in this precipitate.

These first results tend to demonstrate the stronger adsorption of bolaamphiphiles comprising a longer hydrophobic chain. Two additional experiments were performed to demonstrate this. First, in situ synthesis of AuNPs was carried out by addition of a $NaBH_4$ solution upon a mixture of bolaamphiphiles and $HAuCl_4$. The sizes of the resulting AuNPs were measured from TEM measurements, and average diameters are reported in Figure 5. Whereas poor size and

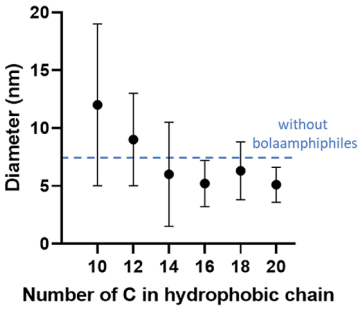

Figure 5. Evolution of the average diameter of AuNPs formed in situ by addition of a $NaBH_4$ solution upon a mixture of bolaamphiphiles and $HAuCl_4$ ($[Au]_{final} = [BolaAla\text{-}C_n] = 5 \times 10^{-4}$ mol·L^{-1}).

dispersity control is obtained for shorter hydrophobic chains (C_{10}–C_{14}), longer hydrophobic chains led to good control over both parameters, which might result from stronger interactions with AuNPs' growth surfaces.

In order to further demonstrate the crucial role of the alky chain length on the interaction level with AuNPs, the catalytic performance of Au@BolaAla-C_n was further studied. While catalytic experiments are a useful tool to characterize the accessibility of the surface of AuNPs, this accessibility can be indirectly related to the level of interactions of these bolaamphiphiles with the nanoparticle surfaces if one keeps the concentration and ionic strength conditions constant. Thus, the reduction of *p*-nitrophenol to *p*-aminophenol in water and in the presence of $NaBH_4$ was performed in the presence of Au@BolaAla-C_n as illustrated in Figure 6.

The kinetic parameters of this model reaction were easily extracted by UV–vis monitoring in pseudo-first-order conditions. Typically, when *p*-nitrophenol in water is mixed with $NaBH_4$, a strong absorbance appears at 400 nm (due to the formation of *p*-nitrophenate), which decreases after the addition of the catalyst. The apparent rate constant (k_{app}) at 25 °C was extracted from the linear relationship between $\ln(A_t/A_0)$ versus the time t.[21] We demonstrate on pristine AuNPs that the apparent velocity constant k_{app} increases linearly with the available area in gold, which is consistent with the data in the literature (Figure S17 in the SI). In the further experiments, the substrate, reductant ($NaBH_4$), and catalyst (AuNPs) concentrations will therefore be set at 10^{-4}, 2×10^{-3}, and 5×10^{-5} mol·L^{-1}, respectively. We determined the k_{app} values for C_{10} and C_{20} chain lengths at 25 °C as depicted in Figure 6B. In these experiments, BolaAla-C_n concentrations were chosen below CAC values to avoid the aggregation phenomenon. Comparatively to pristine AuNPs, the addition of an increasing quantity of bolaamphiphiles tends to decrease the measured value of k_{app}. This effect might be ascribed to the lower accessibility of the AuNPs surface due to an increasing coverage level of the surface. Moreover, whatever the

https://doi.org/10.1021/acs.jpcc.2c01545
J. Phys. Chem. C 2022, 126, 11051–11057

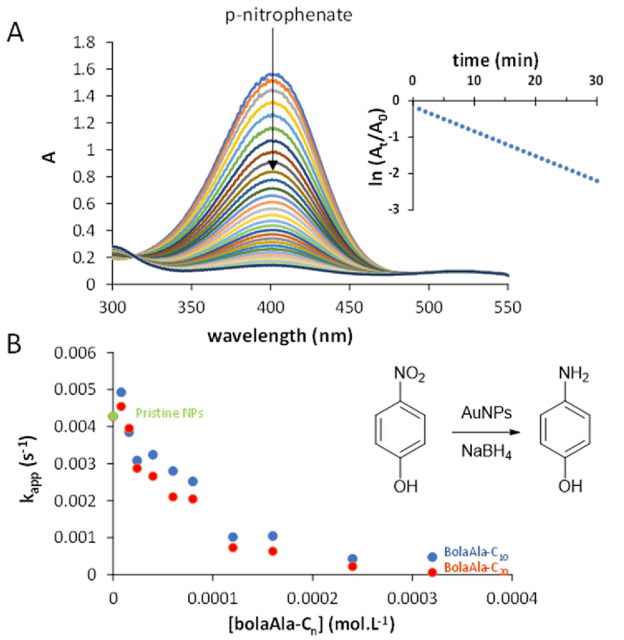

Figure 6. (A) Time dependence of UV−vis absorption spectra for *p*-nitrophenol reduction (10^{-4} mol·L^{-1}) by an excess of $NaBH_4$ (2×10^{-3} mol·L^{-1}) in the presence of AuNPs (5×10^{-4} mol·L^{-1}) and the corresponding linear relationship between $\ln(A/A_0)$ versus time. (B) Plot of the apparent rate constant versus concentrations of [BolaAla-C_{10}] and [BolaAla-C_{20}].

concentration used was, a lower catalytic activity was obtained for nanohybrids stabilized by BolaAla-C_{20} comprising a longer alkyl chain. Therefore, the observed decrease in catalytic activity emphasizes the higher strength of interactions between surfactants and AuNPs promoted by a longer alkyl chain length. To confirm these results, further kinetic measurements were performed as a function of temperature (from 20 to 40 °C) and were then fitted to the Arrhenius equation to obtain the activation energy plot. Activation energy values of 59.5 ± 1.0 and 61.5 ± 1.0 kJ mol^{-1} were found for BolaAla-C_{10} and BolaAla-C_{20}, respectively, while it was 40.5 ± 1 kJ mol^{-1} for the pristine NPs. Finally, the Au@BolaAla-C_{20} catalytic system can be precipitated at the end of the reaction (by addition of HCl or by bubbling CO_2), whereas for pristine AuNPs and Au@BolaAla-C_{10}, precipitation is irreversible (see Figures S18−S20 in the SI). The precipitated catalyst can be easily recovered by returning to a higher pH (by addition of a NaOH base or by bubbling N_2) for further use of the catalyst. Interestingly, using a CO_2/N_2 recycling process prevents the formation of salt (and an increase in ionic strength) and promotes a higher recyclability of catalyst systems (see Figure S21).

4. CONCLUSIONS

In conclusion, bolaamphiphilic-type structures can be effective substitutes to conventional surfactants for the stabilization of interfaces. To demonstrate this effect, different families of bolaamphiphilic structures comprising different polar heads (amine and carboxylate) and hydrophobic chains of various lengths (C_{10}−C_{20}) were synthesized and used to study the interactions with gold surfaces in water. As expected, the proper choice of polar heads is a prerequisite to obtain a satisfactory level of interactions with alanine heads leading to better results for a chosen chain length among the studied systems. In addition, the choice of sufficiently long hydrophobic structures (above C_{14}) allows us not only to control the growth of AuNPs and their catalytic activity but also to improve the stabilization properties of the obtained particles. Interactions between hydrophobic chains dramatically strengthen the interactions with NP surfaces. Hence, for alanine-terminated bolaamphiphiles, a reversible aggregation process is observed for the longer hydrophobic chains related to the ability of these molecules to form fibrillar structures with AuNPs trapped within at low pH values.

This work opens up new perspectives, in particular on the understanding of the growth mechanisms of nanoparticles. In particular, it highlights the critical effect of the length of the hydrophobic part of the growth/stabilization agents used, which modulates the strength of the interaction with the growth interface. This point could in particular be used to promote anisotropic growth phenomena widely studied in the literature.[1,2,4] Lastly, all these studies were performed well below the critical aggregation concentration of these molecules. Further studies will evaluate its additional effect on the stabilization of solid−liquid interfaces.

■ ASSOCIATED CONTENT

Supporting Information

The Supporting Information is available free of charge at https://pubs.acs.org/doi/10.1021/acs.jpcc.2c01545.

Additional information concerning the synthesis and characterization of bolaamphiphiles, their self-assemblies' properties in solution, the synthesis and characterization of preformed AuNPs, and the study of their catalytic properties (PDF)

■ AUTHOR INFORMATION

Corresponding Authors

Nancy Lauth-de Viguerie − *IMRCP, Université de Toulouse, CNRS UMR 5623 Université Toulouse III − Paul Sabatier, F-31062 Toulouse, France*; Email: nancy.de-viguerie@univ-tlse3.fr

Jean-Daniel Marty − *IMRCP, Université de Toulouse, CNRS UMR 5623 Université Toulouse III − Paul Sabatier, F-31062 Toulouse, France*; orcid.org/0000-0001-7631-8865; Email: jean-daniel.marty@univ-tlse3.fr

Authors

Stéphanie Sistach − *IMRCP, Université de Toulouse, CNRS UMR 5623 Université Toulouse III − Paul Sabatier, F-31062 Toulouse, France*

Elodie Marinoni − *IMRCP, Université de Toulouse, CNRS UMR 5623 Université Toulouse III − Paul Sabatier, F-31062 Toulouse, France*

Christophe Mingotaud − *IMRCP, Université de Toulouse, CNRS UMR 5623 Université Toulouse III − Paul Sabatier, F-31062 Toulouse, France*; orcid.org/0000-0002-9651-6209

Complete contact information is available at: https://pubs.acs.org/10.1021/acs.jpcc.2c01545

Author Contributions

The manuscript was written through contributions of all authors. All authors have given approval to the final version of the manuscript.

Notes

The authors declare no competing financial interest.

■ ACKNOWLEDGMENTS

The authors thank the Université de Toulouse and CNRS for funding.

■ ABBREVIATIONS

AuNP:gold nanoparticle; CAC:critical aggregation concentration; NPs:nanoparticles; TEM:transmission electron microscopy

■ REFERENCES

(1) Perezjuste, J.; Pastorizasantos, I.; Liz-Marzan, L.; Mulvaney, P. Gold nanorods: Synthesis, characterization and applications. *Coord. Chem. Rev.* **2005**, *249*, 1870−1901.
(2) Zheng, J.; Cheng, X.; Zhang, H.; Bai, X.; Ai, R.; Shao, L.; Wang, J. Gold Nanorods: The Most Versatile Plasmonic Nanoparticles. *Chem. Rev.* **2021**, *121*, 13342−13453.
(3) Yuan, C.; Jiang, J.; Wang, D.; Hu, Y.; Liu, M. In Situ Growth of Chiral Gold Nanoparticles in Confined Silica Nanotube. *J. Nanosci. Nanotechnol.* **2019**, *19*, 2789−2793.
(4) Jiang, J.; Wang, T.; Liu, M. Creating chirality in the inner walls of silica nanotubes through a hydrogel template: chiral transcription and chiroptical switch. *Chem. Commun.* **2010**, *46*, 7178−7180.
(5) Paczesny, J.; Wójcik, M.; Sozański, K.; Nikiforov, K.; Tschierske, C.; Lehmann, A.; Górecka, E.; Mieczkowski, J.; Hołyst, R. Self-Assembly of Gold Nanoparticles into 2D Arrays Induced by Bolaamphiphilic Ligands. *J. Phys. Chem. C* **2013**, *117*, 24056−24062.
(6) Sistach, S.; Rahme, K.; Pérignon, N.; Marty, J.-D.; Lauth-deViguerie, N.; Gauffre, F.; Mingotaud, C. Bolaamphiphile Surfactants as Nanoparticle Stabilizers: Application to Reversible Aggregation of Gold Nanoparticles. *Chem. Mater.* **2008**, *20*, 1221−1223.
(7) Wu, Z. D. Preparation of Gold Nanoparticles by Using Cholesteryl Compounds. *Appl. Mech. Mater.* **2013**, *368-370*, 795−798.
(8) Jiao, T.; Wang, Y.; Guo, W.; Zhang, Q.; Yan, X.; Chen, J.; Wang, L.; Xie, D.; Gao, F. Synthesis and photocatalytic property of gold nanoparticles by using a series of bolaform Schiff base amphiphiles. *Mater. Res. Bull.* **2012**, *47*, 4203−4209.
(9) Wang, F. Y.; Jiao, T. F. Synthesis of Gold Nanoparticles by Using a Bolaform Schiff Base Amphiphile at Liquid-Liquid Interface. *Adv. Mater. Res.* **2012**, *490-495*, 3694−3697.
(10) Jiao, T.; Wang, Y.; Zhang, Q.; Yan, X.; Chen, J.; Zhou, J.; Gao, F. Preparation and Photocatalytic Property of Gold Nanoparticles by Using Two Bolaform Cholesteryl Imide Derivatives. *J. Dispersion Sci. Technol.* **2013**, *34*, 1675−1682.
(11) Yin, Y.; Alivisatos, A. Colloidal nanocrystal synthesis and the organic−inorganic interface. *Nature* **2005**, *437*, 664−670.
(12) *Purification of laboratory chemicals,* 8th ed., Armarego, W. L. F. Ed., Elsevier: Paris, 2017,
(13) Franceschi, S.; Lauth-de Viguerie, N.; Riviere, M.; Lattes, A. Synthesis and aggregation of two-headed surfactants bearing amino acid moieties. *New J. Chem.* **1999**, *23*, 447−452.
(14) Menger, F. M.; Wrenn, S. Interfacial and Micellar Properties of Bolaform Electrolytes. *J. Phys. Chem.* **1974**, *78*, 1387−1390.
(15) Jablonkai, I.; Oroszlan, P. Preparation of ω-functionalized eicosane-phosphate building blocks. *Chem. Phys. Lipids* **2005**, *133*, 103−112.
(16) Fainerman, V. B.; Lucassen-Reynders, E. H.; Miller, R. Adsorption of surfactants and proteins at fluid interfaces. *Colloids Surf., A* **1998**, *143*, 141−165.
(17) Weisbecker, C. S.; Merritt, M. V.; Whitesides, G. M. Molecular Self-Assembly of Aliphatic Thiols on Gold Colloids. *Langmuir* **1996**, *12*, 3763−3772.
(18) Mayya, K. S.; Patil, V.; Sastry, M. On the Stability of Carboxylic Acid Derivatized Gold Colloidal Particles: The Role of Colloidal Solution pH Studied by Optical Absorption Spectroscopy. *Langmuir* **1997**, *13*, 3944−3947.
(19) Rahme, K.; Gauffre, F.; Marty, J.-D.; Payré, B.; Mingotaud, C. A Systematic Study of the Stabilization in Water of Gold Nanoparticles by Poly(Ethylene Oxide)−Poly(Propylene Oxide)−Poly(Ethylene Oxide) Triblock Copolymers. *J. Phys. Chem. C* **2007**, *111*, 7273−7279.
(20) Yon, M.; Pibourret, C.; Marty, J.-D.; Ciuculescu Pradines, D. Easy colorimetric detection of gadolinium ions based on gold nanoparticles: key role of phosphine-sulfonate ligands. *Nanoscale Adv.* **2020**, *2*, 4671−4681.
(21) Yin, F.; Nguyen, H. H.; Coutelier, O.; Destarac, M.; Lauth-de Viguerie, N.; Marty, J.-D. Effect of copolymer composition of controlled (N-vinylcaprolactam/N-vinylpyrrolidone) statistical copolymers on formation, stabilization, thermoresponsiveness and catalytic properties of gold nanoparticles. *Colloids Surf., A* **2021**, *630*, No. 127611.

https://doi.org/10.1021/acs.jpcc.2c01545
J. Phys. Chem. C 2022, 126, 11051−11057